Chapter 5

Influence of loading and loading-free processes of cyclic torsional shear to soil compaction

5.1 Introduction

In the previous chapters, the soil behavior related to traffic-induced loading system has been discussed to some extent by adopting the cyclic torsional shear loading method. The interrelationships between factors involved in soil behavior, failure characteristics and dynamic shear strength have been clarified. These studies focused on the behavior of soil during loading application. However, in fact, during crop production soil is not subjected to machinery loading all of the time. It is mechanically loaded during the periods of machinery services including tillage, spraying herbicide or pesticide, fertilizing and harvesting, and is in the condition of being free of machinery loading during the remaining periods. Soil behavior induced by this specific loading pattern might be different from that of the continuous loading one that was reported in the previous chapters.

In this chapter, therefore, the investigations have been carried out in order to discuss soil behavior induced by this specific loading system. The cyclic torsional shear loading served as a tool of simulation of the loading system during machinery field services, emphasizing torsional shear phenomena, i.e. turning, driving on irregular field profile and hillside operation. On the other hand, the loading-free process with allowance for the dissipation of pore water pressure was taken into consideration incorporating the remaining periods of no machinery excitation. This specific behavior of soil for this loading system was investigated and discussion was made based on the interrelationships among major factors including the stress, strain, pore water pressure, bulk density, and

number of cyclic loading.

5.2 Methodology

Preparation of the soil specimens and the test method followed the procedures described in Chapter 3 up to the consolidation process. Then, the loading and loading-free processes of cyclic torsional shear were applied to the specimen. This loading pattern is demonstrated in Fig. 5.1. It was composed of series of loading set. One loading set was a combination of cyclic loading process and a loading-free one. First, cyclic torsional shear load was applied to soil specimens for a certain period of Nc; this process was called the

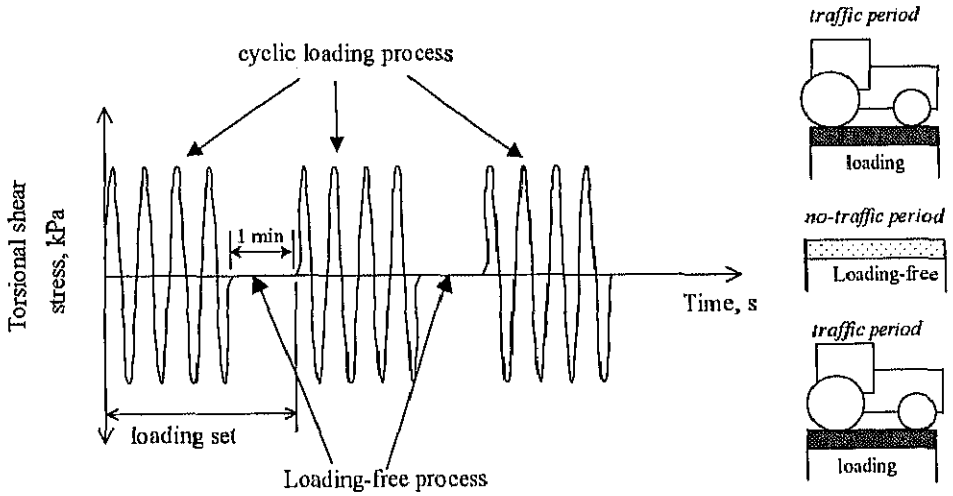

Fig. 5.1 Loading pattern.

cyclic loading process. Then, the cyclic load was removed and drainage was performed to allow dissipation of the build-up pore water pressure during the cyclic loading process. This process was referred to as the loading-free process. The cyclic loading process was considered to simulate the traffic period during machinery services. On the other hand, the loading-free process corresponded to the no-traffic period in the field. During the cyclic

loading process, the soil specimen was exposed under undrained condition. This was based on the fact that there is less time to let drainage occur during machinery traffic. However, after being free from traffic the drainage in soil will occur and the soil will change to another stable state. Therefore, the drainage was allowed solely during the loading-free process.

The test combinations are listed in Table 5.1. The studies in the previous chapters suggested that no significant effect of loading frequency was recognized on soil behavior under cyclic torsional shear loading. Accordingly, the loading frequency was not taken into consideration in the design of test combinations. All tests were conducted at 0.2 Hz.

Table 5.1 Test combinations

Test No.	$\tau_{z\theta}$, kPa	ρ, Mg/m^3	Nc in loading set
1	14.9	0.99	4
2	17.0	1.00	4
3	19.0	1.01	4
4	14.9	0.82	4
5	14.9	0.90	4
6	14.9	1.00	8

5.3 Results and discussion

5.3.1 Dynamic soil responses

Typical corresponding results under the loading pattern in Fig. 5.1 are shown in Figs. 5.2 and 5.3 in terms of torsional shear strain and pore water pressure against the

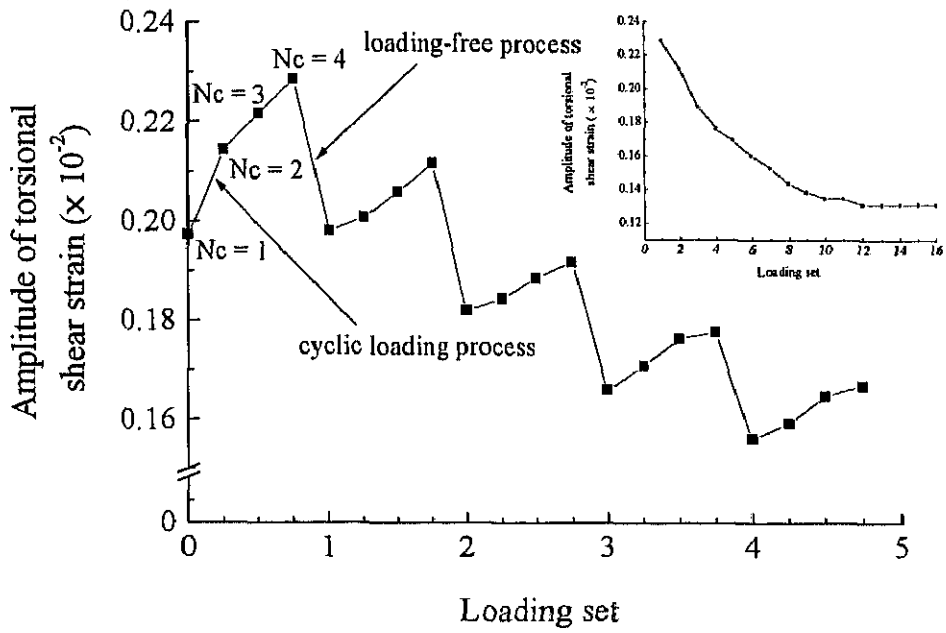

Fig. 5.2 Amplitude of torsional shear strain versus loading set.

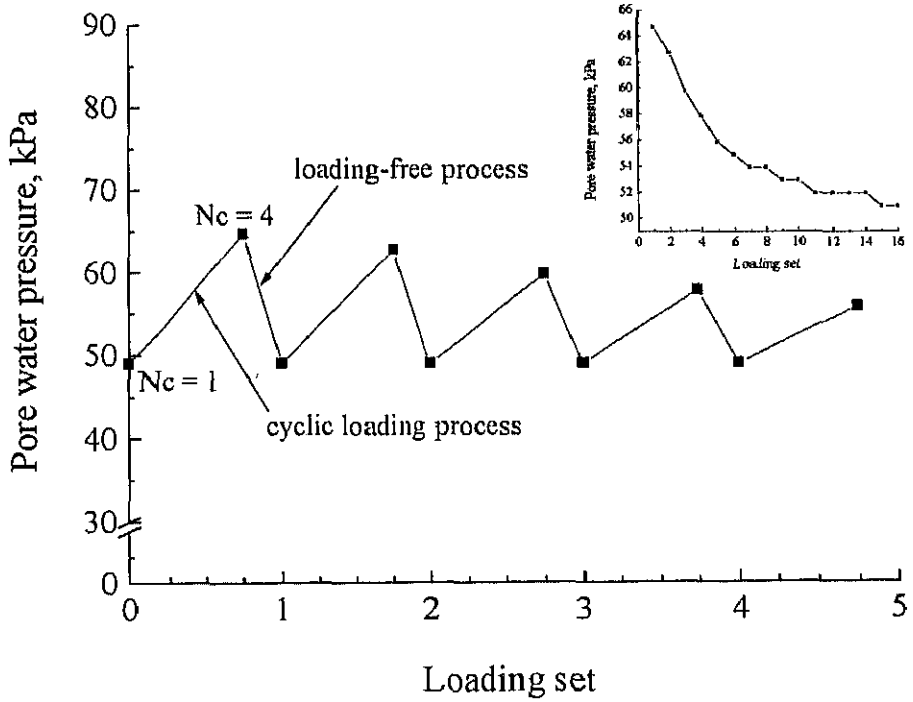

Fig. 5.3 Pore water pressure versus loading set.

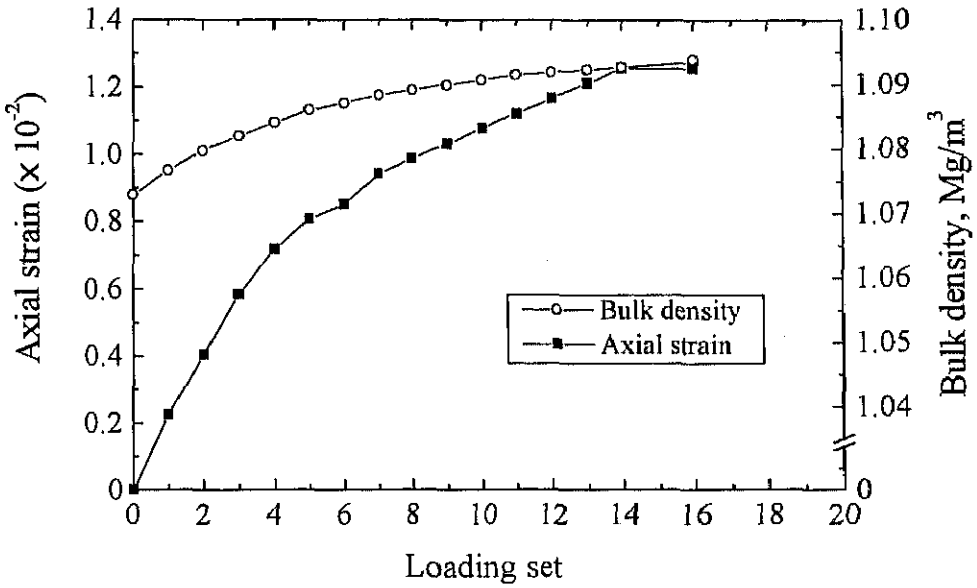

Fig. 5.4 Axial strain and bulk density versus loading set.

loading set, respectively. The test was carried out using the specimen of 1.0 Mg/m^3 with loading magnitude of 14.9 kPa and loading frequency of 0.2 Hz. The loading set included the cyclic loading process with Nc = 4 and the loading-free process. On the average, for all tests, it took about 1 min. to complete the loading-free process that was indicated by a constant state of pore water pressure. Figs. 5.2 and 5.3 represent the results at the initial period. However, the complete results for this test were provided by reduced figures placed inside each figure. In these figures, the values of torsional shear strain and pore water pressure were observed at the last loading cycle (Nc = 4) on the cyclic loading process of each loading set.

When the first loading set was applied, the torsional shear strain and pore water pressure increased with the increase of Nc during the cyclic loading process. After removal of the cyclic load and succeeding initiation of the loading-free process, pore water pressure decreased to nearly its initial value under the given confining pressure. Consequently, the

soil specimen was compacted more and became stiffer as can be seen in Fig. 5.4. This figure shows the amounts of axial strain and bulk density at the end of each loading set. It is necessary to note that torsional shear strain was developed during the cyclic loading process whereas axial strain and bulk density were discerned under the loading-free process. The soil specimen was first compacted in the consolidation process before the loading set was initiated. This compaction state was evident in Fig. 5.4 as the initial value of bulk density, which was about 1.072 Mg/m^3 in this case.

After the loading sets were continued, the increases of torsional shear strain and pore water pressure during the cyclic loading process were comparatively lower than that of the preceding loading set. Accordingly, the overall values of the strain and the pore water exhibited decreasing trends as shown by the reduced figures in Fig. 5.2 and 5.3, respectively. Also, the increasing rates of bulk density and axial strain were greater at the initial period and became lower afterwards. This might be due to stiffening of the soil

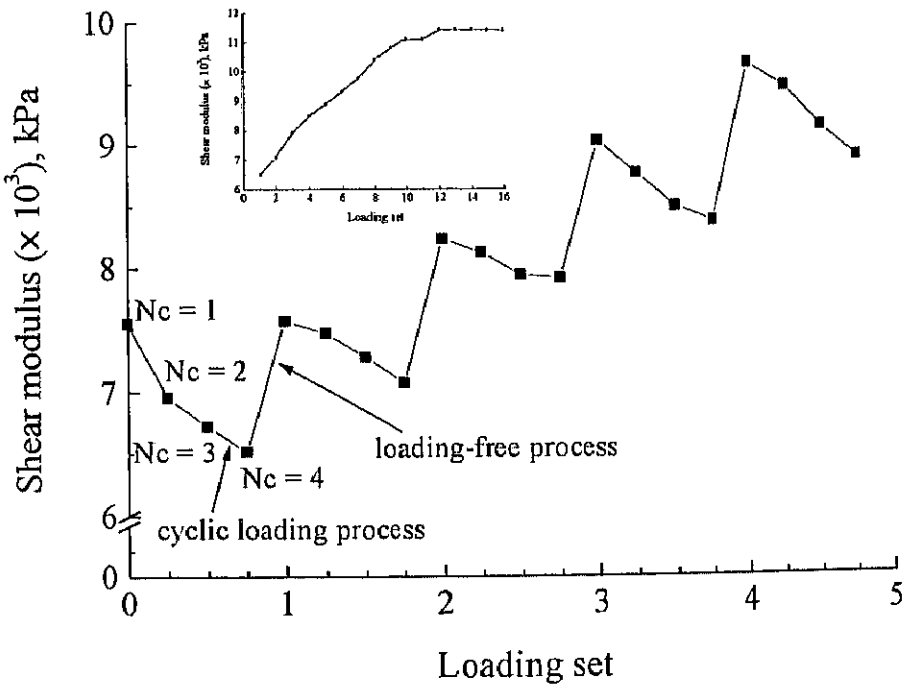

Fig. 5.5 Shear modulus versus loading set.

specimen.

Stiffening of the soil specimen can also be recognized by the value of shear modulus in Fig. 5.5. Shear modulus of the soil specimen decreased due to excitation during the cyclic loading process but increased during the loading-free process because of additional compaction of the soil specimen. The overall value of shear modulus increased and seemed to remain constant when the loading set advanced in the range up to 12 as shown by the reduced figure inside Fig. 5.5. Similar characteristics were also found for torsional shear strain, pore water pressure, and axial strain and bulk density in Figs. 5.2, 5.3 and 5.4, respectively. This implies that the soil specimen seemed to reach a stable state at this range of loading set.

The bulk density at this range was about 1.094 Mg/m^3. This value could be called a maximum bulk density under this specific loading condition. After this specific loading test finished, bulk density was relatively increased by 2.1% from the initial value of 1.072 Mg/m^3 to a stable state of 1.094 Mg/m^3.

These test results may contribute to the understanding and prediction of soil compaction that is produced by machinery services. It may be useful for making a decision of subsoiling to loosen the subsoil layer. Moreover, this knowledge should be needed for a no-tillage system or related cultivation system that sometimes plowing must be performed to release undesired compaction. Based on these results, it is possible to predict a maximum bulk density induced by machinery services and the time when it will occur. However, further experiments in both the indoor laboratory and the actual field situation are needed to establish the prediction approach with high applicability.

5.3.2 Comparison with cyclic torsional shear loading test

Soil specimens under these loading and loading-free processes of cyclic torsional

shear (LFCTS) test behaved differently from one under a normal cyclic torsional shear loading (CTSL) test. The main difference existed in the loading-free process because it allowed soil rebound and transition to another stable state. Fig. 5.6 demonstrates the results of two loading modes. It is notable that the result of torsional shear strain for LFCTS was plotted against Nc instead of loading set for the convenience of visual comparison.

Both tests were conducted under the same setting condition. While torsional shear strain in the CTSL test increased with the increase of Nc until soil failure occurred at Nc = 17, it decreased in the LFCTS test (Fig. 5.6). Even though torsional shear strain of LFCTS also increased along with the one of CTSL in the first 4 cycles, it eventually started to decrease after the loading-free process was applied. Yet, it increased again in the succeeding loading set, but the increased amount was lower owing to stiffening of the soil specimen during the loading-free process. Hence, unlike the CTSL test, the soil specimen under the LFCTS will become denser and not encounter a failure state unless a higher

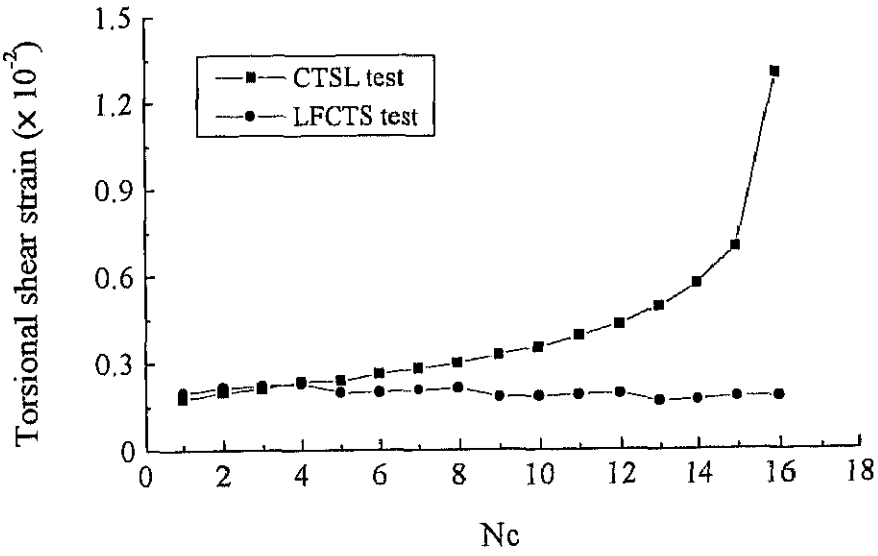

Fig. 5.6 Torsional shear strain versus Nc.

loading magnitude is introduced.

The results of shear modulus for both tests are shown in Fig. 5.7. With the increase of Nc, shear modulus decreased in the CTSL test while it increased in the LFCTS test. This indicated changes of stiffness in the soil during the tests. Cyclic stiffness decreased in both tests when cyclic loading was applied. However, the stiffness became higher during the loading-free process in the LFCTS test and then its overall value showed an increasing trend.

The LFCTS test seems to be capable for the prediction of soil behavior during the whole period of crop production since it provides both loading and loading-free processes to the soil while the CTSL test might be suitable to simulate soil behavior during the time when machines are operating. The results of the LFCTS test were shown with only few numbers of Nc in Figs. 5.6 and 5.7 in order to represent a clear difference between both test modes.

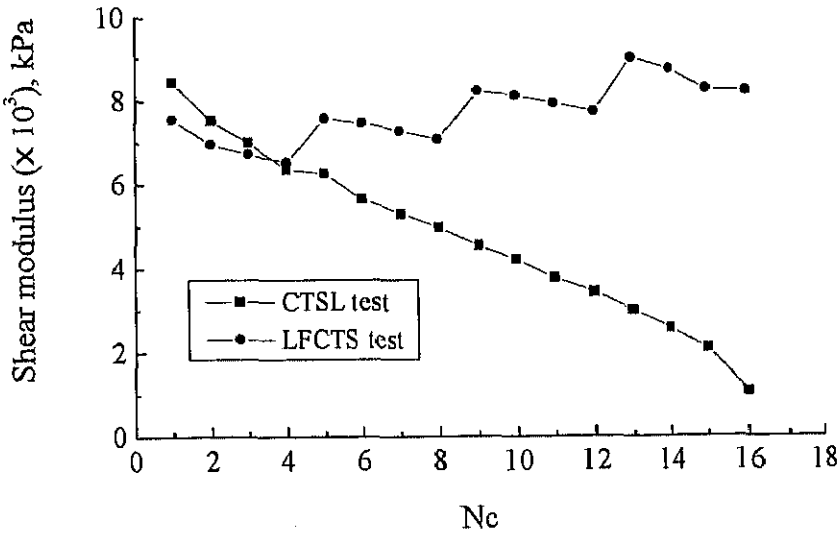

Fig. 5.7 Shear modulus versus Nc.

5.3.3 Effects of loading magnitude, Nc and bulk density

As reported by previous works[13),11),35)], some factors including the dynamic load and numbers of wheel passes are instrumental. The effects caused by these factors were also taken into account in this test under various loading combinations as shown in Figs. 5.8, 5.9 and 5.10. It was found that higher loading magnitude given during the cyclic loading process of loading set yielded higher torsional shear strain (Fig. 5.8(a)). Besides, it resulted in higher axial strain and increase of bulk density during the loading-free process of loading set (Fig. 5.8(b) and 5.8(c)). It was found that the change of the soil specimen during the cyclic loading process affected the soil behavior during the loading-free process. Yasuhara *et al.*[96] reported in the study of post-cyclic recompression settlement that the development of pore water pressure during cyclic loading had an effect on additional volumetric strain during re-consolidation after the cyclic loading process. It was deduced that the higher the pore water pressure produced during cyclic loading, the more increase of additional volumetric strain was obtained. The changes of bulk density under the loading-free process in this test might also be related to this cause. As shown in Fig. 5.11, the higher loading magnitude produced higher pore water pressure. This figure presented pore water pressure against the loading set for various loading combinations including loading magnitude, loading frequency and bulk density.

For the loading set with the cyclic loading process conducted for different Nc of 4 and 8, the results of torsional shear strain were not much different, although it was larger in the loading set with higher Nc (Fig. 5.9(a)). However, the results of pore water pressure in Fig. 5.11 were considerably different. This may help explain the significant difference in the axial strain and bulk density in Figs. 5.9(b) and 5.9(c). Hence, it could be confirmed that the pore water pressure developed during the cyclic loading process had an effect on

subsequent soil behavior during the loading-free process.

The results regarding the effect of bulk density are shown in Fig. 5.10. Additionally, the changes in whole values of bulk density during the loading set are also included in this figure (Fig. 5.10(d)). It was found that the amounts of torsional shear strain, axial strain and increase of bulk density were higher in specimens having lower bulk density. Moreover, it is interesting to note that these values for bulk density of 0.8 Mg/m^3 were so much higher than those of 0.9 and 1.0 Mg/m^3 (Fig. 5.10). The cause may come from the fact that the test for the bulk density of 0.8 Mg/m^3 was a unique case in which failure was encountered during the first loading set. Fig. 5.12 shows the results of this test at the initial loading period in terms of torsional shear strain and shear modulus. The soil specimen failed at Nc = 2 during the cyclic loading process of the first loading set as indicated by the large development of torsional shear strain and decrease of shear modulus. However, when the test was continued with strain softening of the specimen until cyclic loading process was complete at Nc = 4, the specimen was restored, becoming stiffer during the loading-free process as indicated by the increase of shear modulus in Fig 5.12. When the second loading set was performed, the soil specimen did not show any sign of failure but still took high torsional shear strain. Eventually, with the increase of the loading set, the soil became stiffer and reached its maximum compaction state with a substantial value of bulk density as shown in Fig. 5.10(c) and (d). Besides, it can be observed that the increase of bulk density was almost produced in the beginning period. As shown in Fig. 5.10(c) at the sixth loading set the increase of bulk density was found to be over 80% of the maximum value.

Based on this result, it is deduced that if soil failure occurs during the loading process of the first loading set, the soil might be loosened and is in the condition of being easy to contract by successive loading sets.

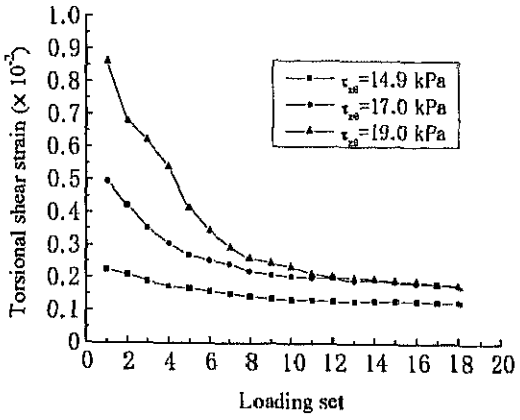

(a)

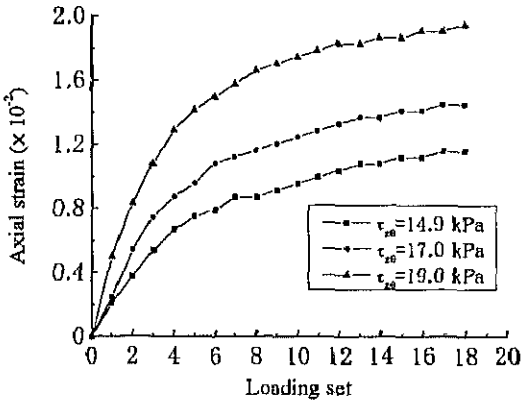

(b)

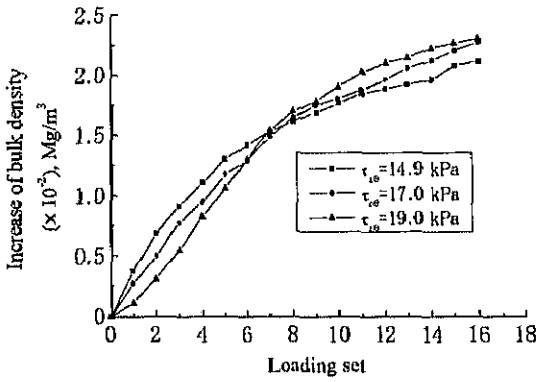

(c)

Fig. 5.8 Effects of loading magnitude (ρ = 1.0 Mg/m^3 and loading set with Nc = 4).

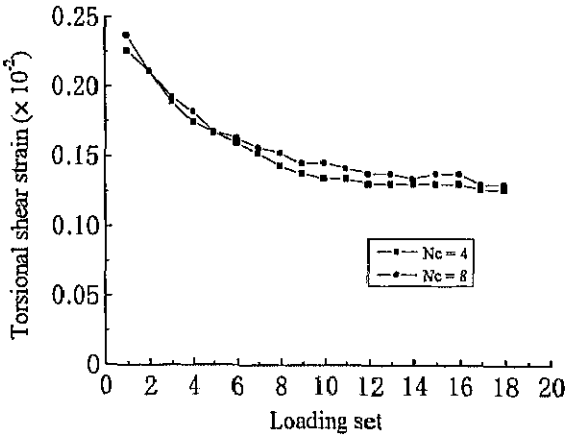

(a)

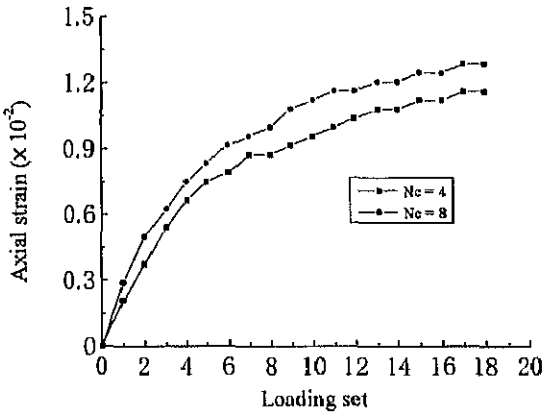

(b)

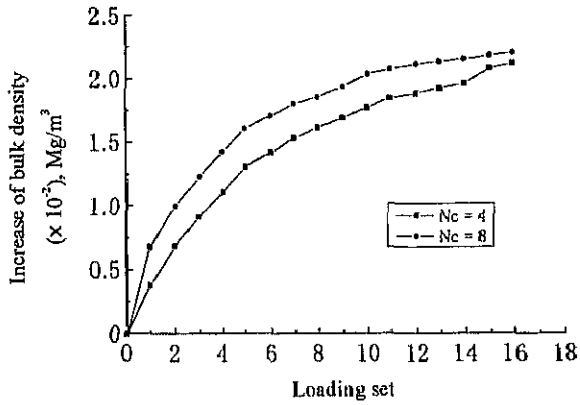

(c)

Fig. 5.9 Effects of number of loading in loading set

($\tau_{z\theta}$ = 14.9 kPa and ρ = 1.0 Mg/m^3).

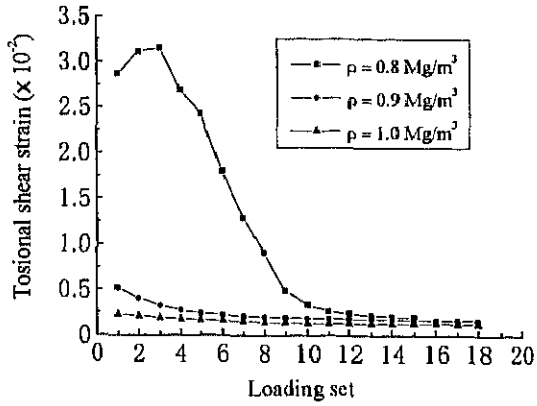
Tosional shear strain (x 10⁻²)
3.5
3.0
2.5
2.0
1.5
1.0
0.5
0
0 2 4 6 8 10 12 14 16 18 20
Loading set
ρ = 0.8 Mg/m³
ρ = 0.9 Mg/m³
ρ = 1.0 Mg/m³

(a)

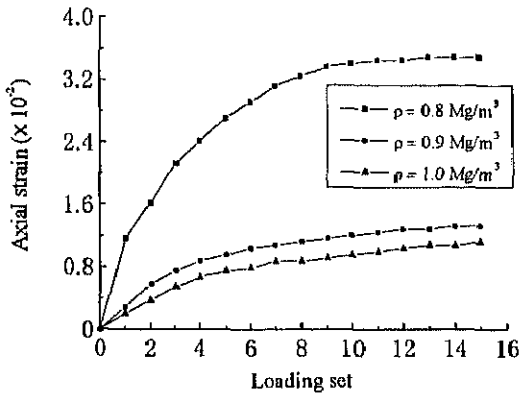
Axial strain (x 10⁻²)
4.0
3.2
2.4
1.6
0.8
0
0 2 4 6 8 10 12 14 16
Loading set
ρ = 0.8 Mg/m³
ρ = 0.9 Mg/m³
ρ = 1.0 Mg/m³

(b)

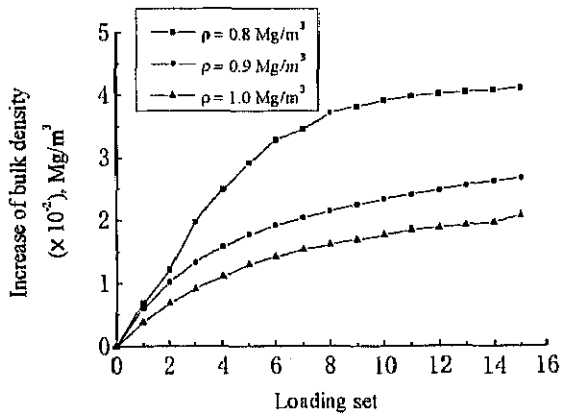
Increase of bulk density
(x 10⁻²), Mg/m³
5
4
3
2
1
0
0 2 4 6 8 10 12 14 16
Loading set
ρ = 0.8 Mg/m³
ρ = 0.9 Mg/m³
ρ = 1.0 Mg/m³

(c)

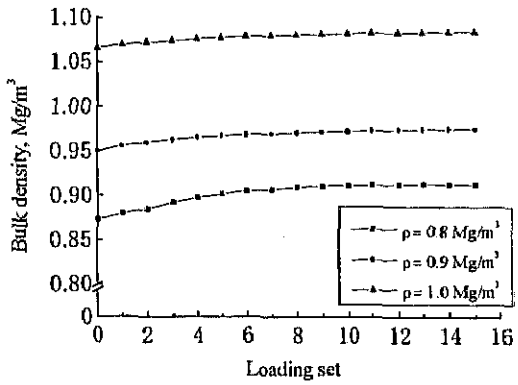

(d)

Fig. 5.10 Effects of bulk density (τ_{z0} = 14.9 kPa and loading set with Nc = 4).

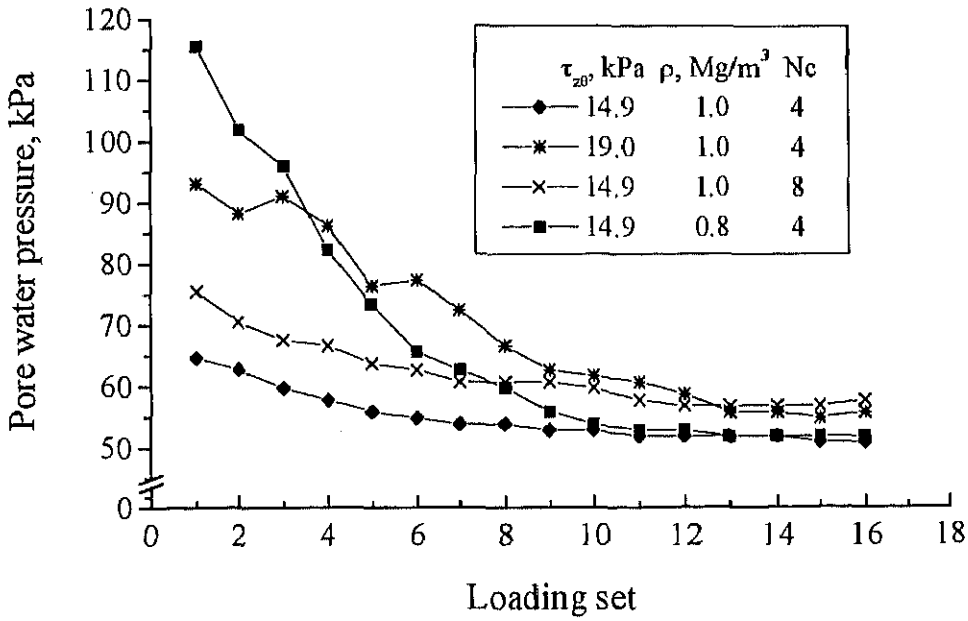

Fig. 5.11 Pore water pressure versus loading set.

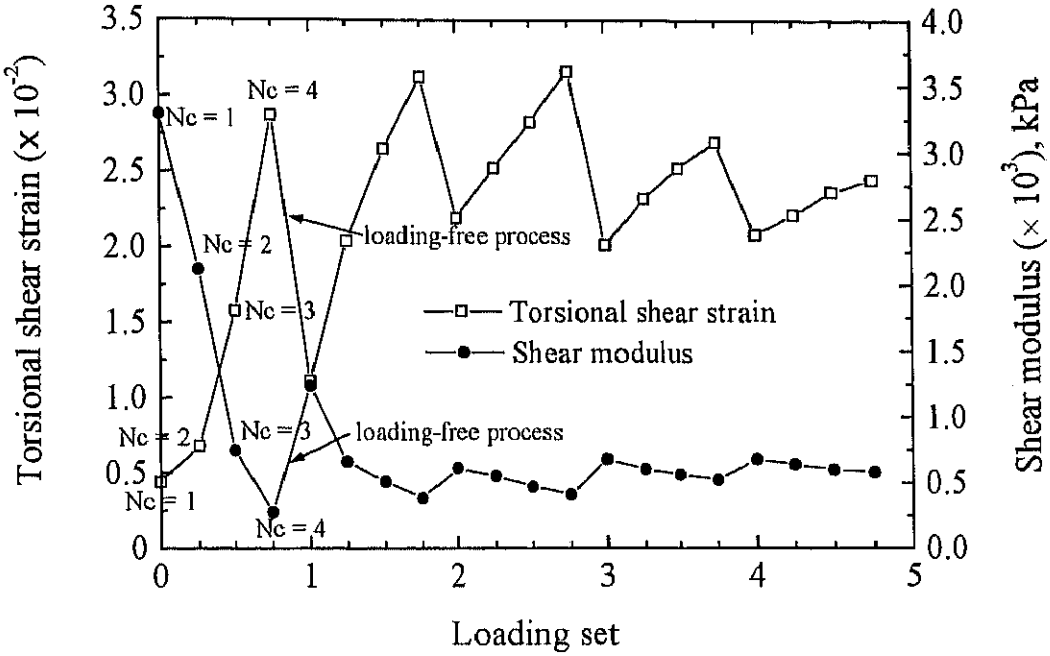

Fig. 5.12 Torsional shear strain and shear modulus versus loading set ($\rho = 0.8$ Mg/m^3).

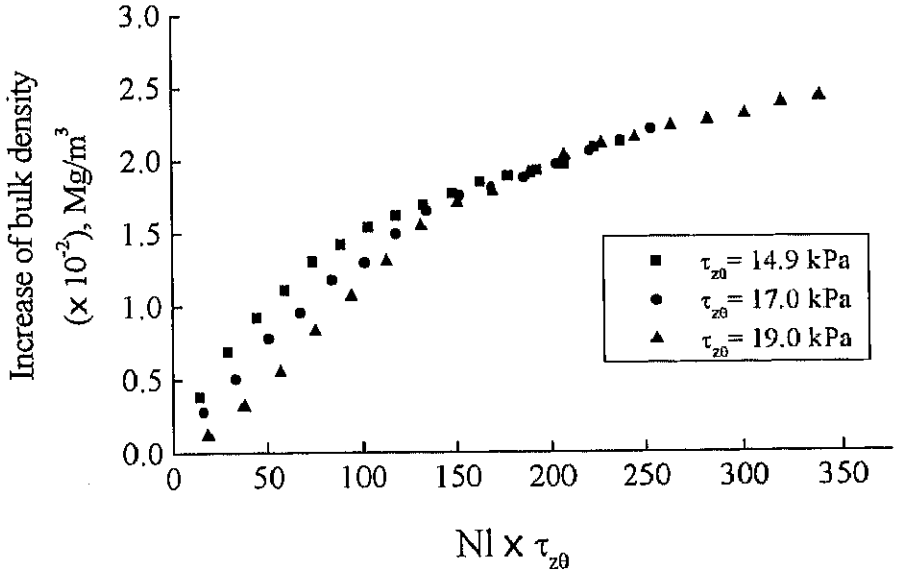

Fig. 5.13 Increment of bulk density versus Nl × $\tau_{z\theta}$ (ρ = 1.0 Mg/m^{3}and Nc = 4).

Further analysis was carried out based on loading intensity with an attempt to establish the general parameter to predict the state of soil compaction during loading and loading-free application. The loading intensity was defined by the number of loading set (Nl) multiplied by cyclic torsional shear stress, $Nl \times \tau_{z\theta}$. Although some measured points were scattered at the beginning period, there was a worthy relationship between $Nl \times \tau_{z\theta}$ and the increase of bulk density (Fig. 5.13). The increase of bulk density seems to be a function of $Nl \times \tau_{z\theta}$. Therefore, in practical use, this may be useful for the prediction of field soil compaction induced by machinery services. However, since it is difficult to interpret the effect of scattering points in the beginning process, the necessity of more experiments must be emphasized for precise interpretation of this data.

5.3.4 Stress path in state space

In order to understand the soil behavior during the loading and loading-free processes of the cyclic torsional shear test, the stress state was observed closely through the change of stress path tracing in the state space. The stress path for this specific test in state space of σ'_c, $\tau_{z\theta}$ and v can be depicted by a rigid curve in Fig. 5.14 while its projections on σ'_c–$\tau_{z\theta}$ plane and σ'_c–v plane are expressed in Fig. 5.15. The stress path started from point-A after the consolidation process. When the loading set was initiated with cyclic loading for Nc = 4, it went up to point-B with a constant magnitude of $\tau_{z\theta}$. It moved along the line of constant v with a decrease of σ'_c due to the undrained condition. After removal of $\tau_{z\theta}$ and the allowance of drainage during the loading-free process, the stress path traced to point-C reverting to its original value of σ'_c but with the decrease of specific volume or increase of bulk density. After other loading sets were continued, similar traces were obtained with a gradual reduction in decrement of σ'_c on the cyclic loading process and v on the loading-free process. Eventually no significant changes of

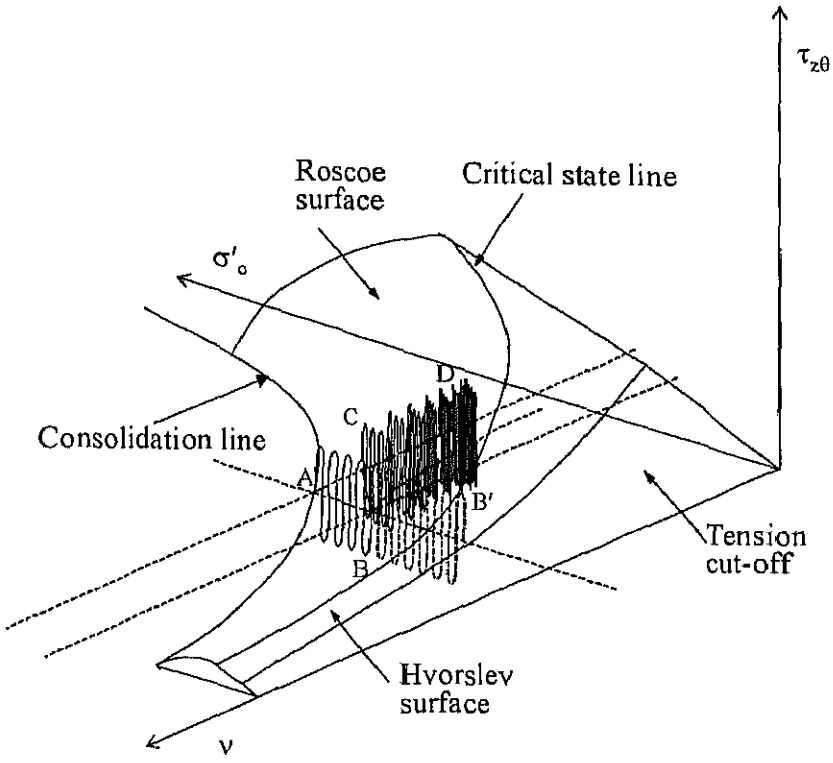

Fig. 5.14 Stress path in state space.

both the decrements of σ'_c and v occurred at higher numbers of loading set as presented at point-D. Correspondingly, the soil specimen obtained a stable state of the loading condition.

As can be seen in the figure, the stress path went towards the critical stress line (CSL) but before touching CSL, $\tau_{z\theta}$ was removed on the way. However, if it was kept fluctuating as represented by the additional dashed curve, it was expected to reach CSL at point-B′ leading to a failure state like the soil characteristics established in the normal cyclic torsional shear loading test. In contrast, under this loading system, the stress path might not meet the CSL or Roscoe surface. The soil specimen may not fail but become denser. This is due to the fact that the soil reaches an another stable state under the same

confining pressure but with a decrease of specific volume. It acquires a larger yield curve on the Roscoe surface and a higher value of critical state so that it cannot reach critical state unless the loading magnitude is increased. This pattern of stress path was recognized for all tests

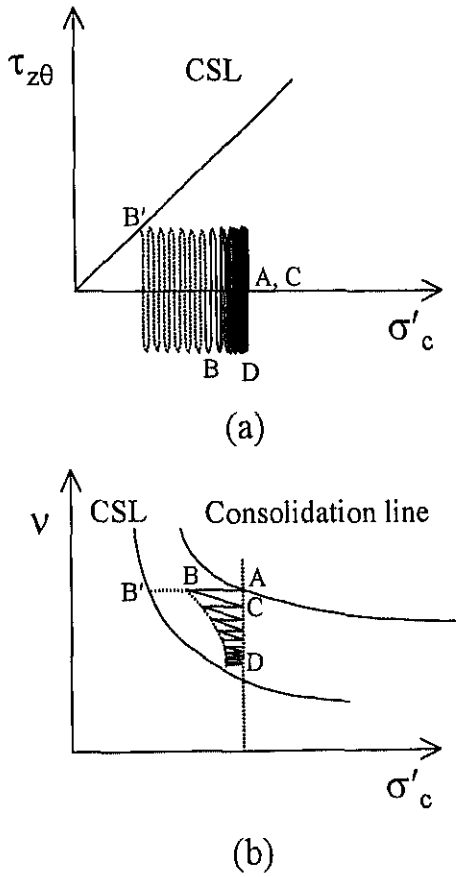

Fig. 5.15 Stress path on (a) σ'_c-$\tau_{z\theta}$ plane and (b) σ'_c-v plane.

5.4 Summary

The loading and loading-free processes of cyclic torsional shear test were conducted to investigate the soil behavior induced by machinery field services. The cyclic

loading process was applied corresponding to the loading system that is generated during machinery operation while the loading-free process simulated the remaining period of no-machinery operation in the field. Based on the test results, corresponding torsional shear deformation was found during the cyclic loading process accompanied by the development of pore water pressure. On the other hand, an increase of bulk density and axial strain occurred during the loading-free process and seemed to be affected by the development of pore water pressure in the preceding cyclic loading process. A comparison with the normal cyclic torsional shear loading test was also made in order to distinguish the soil behavior under both loading modes. Moreover, the effects of loading magnitude, amount of Nc in the loading set and bulk density were clarified. Also, the stress path tracing on the state space was investigated to help explain the soil behavior under loading and loading-free processes. It is deduced that under this specific loading, the soil specimens did not reach failure state but became denser.